Supporting Information for "Cavity quantum-electrodynamical time-dependent density functional theory within Gaussian atomic basis. II. Analytic energy gradient"

(4 March 2022)

S1. THEORY

A. Notations

1. *Some Basic Quantities in Quantum Chemistry*

For a molecule, lowercase Greek letters $\mu, \nu, \lambda, \sigma$, and ρ are used to index atomic orbitals (AO). And we use indices i, j to represent its occupied Kohn-Sham orbitals, and a, b to denote its unoccupied (virtual) Kohn-Sham orbitals. The corresponding orbital energies will be written as $\varepsilon_i, \varepsilon_j, \varepsilon_a$, and ε_b. N_{bas} denotes the number of atomic basis functions, while N_{o} and N_{v} denote the number of occupied and virtual molecular orbitals, respectively. $\mathbf{C}_{\mathrm{o}}$ is a $N_{\mathrm{bas}} \times N_{\mathrm{o}}$ matrix and contains occupied orbital coefficients, $C_{\mu i}$. Similarly, $\mathbf{C}_{\mathrm{v}}$ is a $N_{\mathrm{bas}} \times N_{\mathrm{v}}$ matrix and contains all virtual orbital coefficients, $C_{\mu a}$. The ground state density matrix is $\mathbf{P}_0 = \mathbf{C}_{\mathrm{o}}\mathbf{C}_{\mathrm{o}}^{\dagger}$, and the corresponding Fock matrix is denoted by $\mathbf{F}$,

$$F_{\mu\nu} = H_{\mu\nu} + \sum_{\lambda\sigma} \Pi_{\mu\nu,\lambda\sigma} P_0^{\lambda\sigma} + F_{\mu\nu}^{\mathrm{xc}} \tag{S1}$$

with $\mathbf{H}$ being the core Hamiltonian and other components defined below.

We use

$$\Pi_{\mu\nu,\lambda\sigma} = (\mu\nu \mid \lambda\sigma) - \alpha_{\mathrm{K}}(\mu\lambda \mid \nu\sigma) \tag{S2}$$

to represent "antisymmetrized" electron repulsion integrals over atomic basis functions, where

$$(\mu\nu \mid \lambda\sigma) = \iint \phi_\mu(\boldsymbol{r})\phi_\nu(\boldsymbol{r}) \frac{1}{|\boldsymbol{r} - \boldsymbol{r}'|} \phi_\lambda(\boldsymbol{r}')\, \phi_\sigma(\boldsymbol{r}')\, \mathrm{d}\boldsymbol{r}\mathrm{d}\boldsymbol{r}' \tag{S3}$$

In Eq. (S2), α_{K} is the ratio of Hartree-Fock exchange for hybrid functionals. For range-separated functionals, the exact exchange term in Eq. (S2) involves an operator that combines short-range and long-range components.

For the exchange-correlation energy component of the KS-DFT energy, $E_{\mathrm{xc}} = \int f_{\mathrm{xc}} \mathrm{d}\mathbf{r}$, the corresponding exchange-correlation matrix is,

$$F_{\mu\nu}^{\mathrm{xc}} = \frac{\partial E_{\mathrm{xc}}}{\partial P^{\mu\nu}} = \int \left(\sum_{\xi} \frac{\partial f_{\mathrm{xc}}}{\partial \xi} \frac{\partial \xi}{\partial P^{\mu\nu}} \right) \mathrm{d}\boldsymbol{r} \tag{S4}$$

where ξ refers to alpha and beta electron densities and their gradient components,

$$\xi \in \{\rho_\sigma, \partial_x\rho_\sigma, \partial_y\rho_\sigma, \partial_z\rho_\sigma\} \quad \sigma \in \{\alpha, \beta\} \tag{S5}$$

Subsequently, for the Kohn-Sham response kernel, the exchange-correlation portion will be represented by[1]

$$\Omega_{\mu\nu,\lambda\sigma}^{\mathrm{xc}} = \frac{\partial F_{\mu\nu}^{\mathrm{xc}}}{\partial P^{\lambda\sigma}} = \int \left(\sum_{\xi,\xi'} \frac{\partial^2 f_{\mathrm{xc}}}{\partial\xi\partial\xi'} \frac{\partial \xi}{\partial P^{\mu\nu}} \frac{\partial \xi'}{\partial P^{\lambda\sigma}} \right) \mathrm{d}\boldsymbol{r} \tag{S6}$$

and the next derivative is

$$\begin{aligned} \Xi_{\mu\nu,\lambda\sigma,\kappa\gamma}^{\mathrm{xc}} &= \frac{\partial \Omega_{\mu\nu,\lambda\sigma}^{\mathrm{xc}}}{\partial P^{\kappa\gamma}} \\ &= \int \left(\sum_{\xi,\xi',\xi''} \frac{\partial^3 f_{\mathrm{xc}}}{\partial\xi\partial\xi'\partial\xi''} \frac{\partial \xi}{\partial P^{\mu\nu}} \frac{\partial \xi'}{\partial P^{\lambda\sigma}} \frac{\partial \xi''}{\partial P^{\kappa\gamma}} \right) \mathrm{d}\boldsymbol{r} \end{aligned} \tag{S7}$$

2. Quantities in TDDFT and cQED-TDDFT Calculations

A and **B** will be used to refer to TDDFT super-matrices,[2–8]

$$A_{ai,bj} = (\epsilon_a - \epsilon_i)\delta_{ab}\delta_{ij} + \Pi_{ai,bj} + \Omega^{\mathrm{xc}}_{ai,bj} \tag{S8}$$

$$B_{ai,bj} = \Pi_{ai,jb} + \Omega^{\mathrm{xc}}_{ai,jb} \tag{S9}$$

where $\Pi_{ai,bj}$ and $\Omega^{\mathrm{xc}}_{ai,jb}$ are MO transformations of supermatrices in Eqs. (S2) and (S6). Within TDDFT, the excitation amplitudes $\mathbf{X} = \{X_{ai}\}$ and the de-excitation amplitudes $\mathbf{Y} = \{Y_{ai}\}$ each contain $N_{\mathrm{v}} \times N_{\mathrm{o}}$ elements. For convenience, amplitudes $\mathbf{X}$ and $\mathbf{Y}$ can alternatively be regarded as 1-dimensional vectors, as in Eqs. (S32), (S33), (S34), and (S36).

For an optical cavity with M photon modes, its α-th mode of frequency is denoted by ω_α and the corresponding fundamental coupling strength by $\boldsymbol{\lambda}_\alpha$.[9–11] For convenience, the inner product of the transition dipole moment of each virtual-occupied pair and the photon field will be written as

$$\lambda^\alpha_{ai} = \boldsymbol{\mu}_{ai} \cdot \boldsymbol{\lambda}_\alpha \tag{S10}$$

where $\boldsymbol{\mu}_{ai}$ is the dipole moment vector in the basis of the molecular orbitals

$$\boldsymbol{\mu}_{ai} = \Big(\langle a|\hat{x}|i\rangle, \langle a|\hat{y}|i\rangle, \langle a|\hat{z}|i\rangle \Big) \tag{S11}$$

Accordingly, the electron-photon coupling is defined as

$$g^\alpha_{ai} = \tilde{g}^\alpha_{ai} = \sqrt{\frac{\omega_\alpha}{2}}\lambda^\alpha_{ai} \tag{S12}$$

and the DSE term is[12,13]

$$\Delta_{ai,bj} = \sum_{\alpha=1}^{M} \lambda^\alpha_{ai}\lambda^\alpha_{bj} \tag{S13}$$

The AO counterparts of these elements are

$$\lambda^\alpha_{\mu\nu} = \boldsymbol{\mu}_{\mu\nu} \cdot \boldsymbol{\lambda}_\alpha \tag{S14}$$

$$g^\alpha_{\mu\nu} = \tilde{g}^\alpha_{\mu\nu} = \sqrt{\frac{\omega_\alpha}{2}}\lambda^\alpha_{\mu\nu} \tag{S15}$$

$$\Delta_{\mu\nu,\lambda\sigma} = \sum_{\alpha=1}^{M} \lambda^\alpha_{\mu\nu}\lambda^\alpha_{\lambda\sigma} \tag{S16}$$

3. Full, Skeleton, and Direct Derivatives

The superscript $[x]$ implies a full/total derivative with respect to the nuclear coordinate x, which includes derivatives of the molecular orbitals. In contrast, the skeleton derivative, $[\tilde{x}]$, does not contain orbital responses.[14–16] For example, for a one-electron operator, $\hat{O}$ (such as the kinetic energy, nuclear-attraction, and electron dipole operators) in MO representation,

$$O_{pq} = \langle \psi_p | \hat{O} | \psi_q \rangle = \sum_{\mu\nu} C^*_{\mu p} O_{\mu\nu} C_{\nu q} \tag{S17}$$

its nuclear derivative $O^{[x]}_{pq}$ can be written as,

$$\begin{aligned} O^{[x]}_{pq} &= \left(O_{pq}\right)^{[\tilde{x}]} + \sum_{ai} \frac{\partial O_{pq}}{\partial \Theta_{ai}} \Theta^{[x]}_{ai} \\ &= \left(O_{pq}\right)^{[\tilde{\tilde{x}}]} + \sum_{\mu\nu} \frac{\partial O_{pq}}{\partial S_{\mu\nu}} S^{[x]}_{\mu\nu} + \sum_{ai} \frac{\partial O_{pq}}{\partial \Theta_{ai}} \Theta^{[x]}_{ai}. \end{aligned} \tag{S18}$$

Here the skeleton derivative, $\left(O_{pq}\right)^{[\tilde{x}]}$ is further split into the overlap derivative, $\mathbf{O}^{\mathbf{S}} \cdot \mathbf{S}^{[x]}$, and the direct derivative (*i.e.* excluding both orbital response and overlap derivative contributions),

$$\left(O_{pq}\right)^{[\widetilde{\tilde{x}}]} = \sum_{\mu\nu} C^*_{\mu p} O^{[x]}_{\mu\nu} C_{\nu q} \tag{S19}$$

In KS-DFT calculation, the direct derivatives can also involve the change in the electron density/gradient, $\xi^{[\widetilde{\tilde{x}}]}$, as well as the derivatives of Becke weights for the numerical integration.

4. Overlap Derivatives

For MO coefficients, the skeleton derivatives contain only overlap derivatives,

$$\mathbf{C}_{\mathrm{o}}^{[\tilde{x}]} = -\frac{1}{2}\mathbf{C}\mathbf{C}^\dagger\mathbf{S}^{[x]}\mathbf{C}_{\mathrm{o}} \tag{S20}$$

$$\mathbf{C}_{\mathrm{v}}^{[\tilde{x}]} = -\frac{1}{2}\mathbf{C}\mathbf{C}^\dagger\mathbf{S}^{[x]}\mathbf{C}_{\mathrm{v}}. \tag{S21}$$

Accordingly, the skeleton derivatives of various density matrices (which can be symmetric or nonsymmetric) are,

$$\begin{aligned}\mathbf{D}^{[\tilde{x}]} = -\frac{1}{2}\mathbf{D}\mathbf{S}^{[x]}\mathbf{C}\mathbf{C}^\dagger - \frac{1}{2}\mathbf{C}\mathbf{C}^\dagger\mathbf{S}^{[x]}\mathbf{D}, \\ \mathbf{D} \in [\mathbf{P}_0, \mathbf{P}_\Delta, \mathbf{R}_X, \mathbf{R}_Y]\end{aligned} \tag{S22}$$

One can then compute their product with a Fock-like matrix ($\boldsymbol{\mathcal{F}}$, which can also be non-symmetric) as

$$\begin{aligned}\mathbf{D}^{[\tilde{x}]} \cdot \boldsymbol{\mathcal{F}} &= -\frac{1}{4}\sum_{\mu\nu,\lambda\sigma} D^{\lambda\mu}\left(S^{[x]}_{\mu\nu} + S^{[x]}_{\nu\mu}\right)\left(\mathbf{C}\mathbf{C}^\dagger\right)^{\nu\sigma}\mathcal{F}_{\lambda\sigma} \\ &\quad - \frac{1}{4}\sum_{\mu\nu,\lambda\sigma}\left(\mathbf{C}\mathbf{C}^\dagger\right)^{\lambda\mu}\left(S^{[x]}_{\mu\nu} + S^{[x]}_{\nu\mu}\right)D^{\nu\sigma}\mathcal{F}_{\lambda\sigma} \\ &= -\frac{1}{4}\sum_{\mu\nu,\lambda\sigma} S^{[x]}_{\mu\nu}\left[D^{\lambda\mu}\mathcal{F}_{\lambda\sigma}\left(\mathbf{C}\mathbf{C}^\dagger\right)^{\nu\sigma} + \left(\mathbf{C}\mathbf{C}^\dagger\right)^{\lambda\mu}\mathcal{F}_{\lambda\sigma}D^{\nu\sigma}\right] \\ &\quad - \frac{1}{4}\sum_{\mu\nu,\lambda\sigma} S^{[x]}_{\nu\mu}\left[D^{\nu\sigma}\mathcal{F}_{\lambda\sigma}\left(\mathbf{C}\mathbf{C}^\dagger\right)^{\lambda\mu} + \left(\mathbf{C}\mathbf{C}^\dagger\right)^{\nu\sigma}\mathcal{F}_{\lambda\sigma}D^{\lambda\mu}\right] \\ &= \mathbf{S}^{[x]} \cdot \mathbf{W}\end{aligned} \tag{S23}$$

where $\mathbf{W}$ is a generalized "energy-weighted density matrix",

$$\mathbf{W} = -\frac{1}{2}\boldsymbol{\Lambda}\mathbf{C}\mathbf{C}^\dagger - \frac{1}{2}\mathbf{C}\mathbf{C}^\dagger\boldsymbol{\Lambda}^\dagger \tag{S24}$$

$$\boldsymbol{\Lambda} = \frac{1}{2}\left(\mathbf{D}^\dagger\boldsymbol{\mathcal{F}} + \mathbf{D}\boldsymbol{\mathcal{F}}^\dagger\right) \tag{S25}$$

5. Orbital Rotations

At first order, the orbital rotations are,

$$\mathbf{C}_{\mathrm{o}} = \mathbf{C}_{\mathrm{o}} - \mathbf{C}_{\mathrm{v}}\boldsymbol{\Theta} \tag{S26}$$

$$\mathbf{C}_{\mathrm{v}} = \mathbf{C}_{\mathrm{v}} + \mathbf{C}_{\mathrm{o}}\boldsymbol{\Theta}^\dagger \tag{S27}$$

Therefore, $\mathbf{D}^{\boldsymbol{\Theta}} \cdot \boldsymbol{\mathcal{F}} = \sum_{\mu\nu} \frac{\partial D^{\mu\nu}}{\partial \Theta_{ai}} \mathcal{F}_{\mu\nu}$ can be found to be

$$\mathbf{P}_0^{\boldsymbol{\Theta}} \cdot \boldsymbol{\mathcal{F}} = -\mathbf{C}_\mathrm{v}^\dagger \left(\boldsymbol{\mathcal{F}} + \boldsymbol{\mathcal{F}}^\dagger \right) \mathbf{C}_\mathrm{o} \tag{S28}$$

$$\begin{aligned} \mathbf{P}_{\boldsymbol{\Delta}}^{\boldsymbol{\Theta}} \cdot \boldsymbol{\mathcal{F}} = \mathbf{X}\mathbf{X}^\dagger \mathbf{C}_\mathrm{v}^\dagger \left(\boldsymbol{\mathcal{F}} + \boldsymbol{\mathcal{F}}^\dagger \right) \mathbf{C}_\mathrm{o} \\ + \mathbf{C}_\mathrm{v}^\dagger \left(\boldsymbol{\mathcal{F}} + \boldsymbol{\mathcal{F}}^\dagger \right) \mathbf{C}_\mathrm{o} \mathbf{X}^\dagger \mathbf{X} \end{aligned} \tag{S29}$$

$$\mathbf{R}_X^{\boldsymbol{\Theta}} \cdot \boldsymbol{\mathcal{F}} = \mathbf{X}\mathbf{C}_\mathrm{o}^\dagger \boldsymbol{\mathcal{F}}^\dagger \mathbf{C}_\mathrm{o} - \mathbf{C}_\mathrm{v}^\dagger \boldsymbol{\mathcal{F}}^\dagger \mathbf{C}_\mathrm{v} \mathbf{X} \tag{S30}$$

$$\mathbf{R}_Y^{\dagger,\boldsymbol{\Theta}} \cdot \boldsymbol{\mathcal{F}} = \mathbf{Y}\mathbf{C}_\mathrm{o}^\dagger \boldsymbol{\mathcal{F}} \mathbf{C}_\mathrm{o} - \mathbf{C}_\mathrm{v}^\dagger \boldsymbol{\mathcal{F}} \mathbf{C}_\mathrm{v} \mathbf{Y} \tag{S31}$$

B. TDDFT-PF Energy and Gradient

1. TDDFT-PF Energy Expression in AO Representation

Based on Eq. (4) of the main text, the TDDFT-PF energy of a molecular system in a microcavity can be written as

$$\begin{aligned} \Omega_\mathrm{TDDFT\text{-}PF} &= \Omega_\mathrm{ele} + \Omega_\mathrm{ele\text{-}ph} + \Omega_\mathrm{ph} + \Omega_\mathrm{dse} \\ &= \begin{bmatrix} \mathbf{X}^\dagger & \mathbf{Y}^\dagger & \mathbf{M}^\dagger & \mathbf{N}^\dagger \end{bmatrix} \begin{bmatrix} \mathbf{A}+\boldsymbol{\Delta} & \mathbf{B}+\boldsymbol{\Delta} & \mathbf{g}^\dagger & \tilde{\mathbf{g}}^\dagger \\ \mathbf{B}+\boldsymbol{\Delta} & \mathbf{A}+\boldsymbol{\Delta} & \mathbf{g}^\dagger & \tilde{\mathbf{g}}^\dagger \\ \mathbf{g} & \mathbf{g} & \boldsymbol{\omega} & 0 \\ \tilde{\mathbf{g}} & \tilde{\mathbf{g}} & 0 & \boldsymbol{\omega} \end{bmatrix} \begin{bmatrix} \mathbf{X} \\ \mathbf{Y} \\ \mathbf{M} \\ \mathbf{N} \end{bmatrix} \end{aligned} \tag{S32}$$

where the electronic, electronic-photon, photon, and dipole self-energy portions of the excitation energy are, (notice that $\mathbf{g} = \tilde{\mathbf{g}}$)

$$\begin{aligned} \Omega_\mathrm{ele} &= \mathbf{X} \cdot \mathbf{A} \cdot \mathbf{X} + \mathbf{Y} \cdot \mathbf{A} \cdot \mathbf{Y} \\ &\quad + \mathbf{X} \cdot \mathbf{B} \cdot \mathbf{Y} + \mathbf{Y} \cdot \mathbf{B} \cdot \mathbf{X} \end{aligned} \tag{S33}$$

$$\begin{aligned} \Omega_\mathrm{ele\text{-}ph} &= (\mathbf{X}+\mathbf{Y}) \cdot \mathbf{g}^\dagger \cdot (\mathbf{M}+\mathbf{N}) \\ &\quad + (\mathbf{M}+\mathbf{N}) \cdot \mathbf{g} \cdot (\mathbf{X}+\mathbf{Y}) \\ &= 2\,(\mathbf{M}+\mathbf{N}) \cdot \mathbf{g}_\mathrm{ao} \cdot (\mathbf{R}_X + \mathbf{R}_Y) \end{aligned} \tag{S34}$$

$$\Omega_\mathrm{ph} = \mathbf{M} \cdot \boldsymbol{\omega} \cdot \mathbf{M} + \mathbf{N} \cdot \boldsymbol{\omega} \cdot \mathbf{N} \tag{S35}$$

$$\begin{aligned} \Omega_\mathrm{dse} &= (\mathbf{X}+\mathbf{Y}) \cdot \boldsymbol{\Delta} \cdot (\mathbf{X}+\mathbf{Y}) \\ &= (\mathbf{R}_X + \mathbf{R}_Y) \cdot \boldsymbol{\Delta}_\mathrm{ao} \cdot (\mathbf{R}_X + \mathbf{R}_Y) \end{aligned} \tag{S36}$$

where the electron-photon and DSE components are already converted into AO representation using the transition density matrices (Eqs. (8) and (9) of the main text) as well as the coupling matrix (Eq. (S15)) and DSE supermatrix (Eq. (S16)).

For convenience, we can further define

$$G_{\mu\nu} = \sum_\alpha (M_\alpha + N_\alpha) g_{\mu\nu}^\alpha \tag{S37}$$

which allow us to write the electron-photon coupling term more compactly as

$$\begin{aligned} \Omega_\mathrm{ele\text{-}ph} &= 2\,(\mathbf{M}+\mathbf{N}) \cdot \mathbf{g}_\mathrm{ao} \cdot (\mathbf{R}_X + \mathbf{R}_Y) \\ &= \sum_{\mu\nu} 2G_{\mu\nu} (R_X^{\mu\nu} + R_Y^{\mu\nu}) \\ &= 2\mathbf{G} \cdot (\mathbf{R}_X + \mathbf{R}_Y) \end{aligned} \tag{S38}$$

The one-electron component of the electronic energy in Eq. (S33) can be cast in the atomic orbital basis as

$$\begin{aligned}\Omega_{\text{ele},1} &= \sum_{ai} \left(X_{ai}^2 + Y_{ai}^2\right)(\varepsilon_a - \varepsilon_i) \\ &= \sum_{abi} \left(X_{ai}X_{bi} + Y_{ai}Y_{bi}\right) F_{ab} \\ &\quad - \sum_{aij} \left(X_{ai}X_{aj} + Y_{ai}Y_{aj}\right) F_{ij} \\ &= \mathbf{P}_\Delta \cdot \mathbf{F}\end{aligned} \tag{S39}$$

which depends on the unrelaxed difference density matrix in Eq. (7) of the main text. Through a similar procedure, the two-electron component of the electronic energy in Eq. (S33) can be written as

$$\begin{aligned}\Omega_{\text{ele},2} &= \sum_{ai,bj} \left(X_{ai}X_{bj} + Y_{ai}Y_{bj}\right)\left[\Pi_{ai,bj} + \Omega^{\text{xc}}_{ai,bj}\right] \\ &\quad + \sum_{ai,bj} \left(X_{ai}Y_{bj} + Y_{ai}X_{bj}\right)\left[\Pi_{ai,jb} + \Omega^{\text{xc}}_{ai,bj}\right] \\ &= \sum_{\mu\nu,\lambda\sigma} \left(R_X^{\mu\nu}R_X^{\lambda\sigma} + R_Y^{\mu\nu}R_Y^{\lambda\sigma}\right)\left[\Pi_{\mu\nu,\lambda\sigma} + \Omega^{\text{xc}}_{\mu\nu,\lambda\sigma}\right] \\ &\quad + \sum_{\mu\nu,\lambda\sigma} \left(R_X^{\mu\nu}R_Y^{\sigma\lambda} + R_Y^{\mu\nu}R_X^{\sigma\lambda}\right)\left[\Pi_{\mu\nu,\lambda\sigma} + \Omega^{\text{xc}}_{\mu\nu,\lambda\sigma}\right] \\ &= \left(\mathbf{R}_X + \mathbf{R}_Y^\dagger\right) \cdot \left(\boldsymbol{\Pi} + \boldsymbol{\Omega}^{\text{xc}}\right) \cdot \left(\mathbf{R}_X + \mathbf{R}_Y^\dagger\right)\end{aligned} \tag{S40}$$

using the electron repulsion integral and exchange-correlation portions of the response kernels defined in Eqs. (S2) and (S6).

2. *TDDFT-PF Energy Gradient*

It should be noted that our TDDFT-PF energy in Eq. (S32) is fully variational to the amplitudes, $\mathbf{X}, \mathbf{Y}, \mathbf{M}$, and $\mathbf{N}$. According to the Hellmann-Feynmann theorem, the net contribution from amplitude derivatives – $\mathbf{X}^{[x]}, \mathbf{Y}^{[x]}, \mathbf{M}^{[x]}$, and $\mathbf{N}^{[x]}$ – to the TDDFT-PF energy gradient would vanish. Namely, from Eq. (S32), the corresponding energy gradient contribution

$$\begin{aligned}&\begin{bmatrix}\mathbf{X}^\dagger & \mathbf{Y}^\dagger & \mathbf{M}^\dagger & \mathbf{N}^\dagger\end{bmatrix}^{[x]} \begin{bmatrix}\mathbf{A}+\boldsymbol{\Delta} & \mathbf{B}+\boldsymbol{\Delta} & \mathbf{g}^\dagger & \tilde{\mathbf{g}}^\dagger \\ \mathbf{B}+\boldsymbol{\Delta} & \mathbf{A}+\boldsymbol{\Delta} & \mathbf{g}^\dagger & \tilde{\mathbf{g}}^\dagger \\ \mathbf{g} & \mathbf{g} & \boldsymbol{\omega} & 0 \\ \tilde{\mathbf{g}} & \tilde{\mathbf{g}} & 0 & \boldsymbol{\omega}\end{bmatrix} \begin{bmatrix}\mathbf{X} \\ \mathbf{Y} \\ \mathbf{M} \\ \mathbf{N}\end{bmatrix} \\ &+ \begin{bmatrix}\mathbf{X}^\dagger & \mathbf{Y}^\dagger & \mathbf{M}^\dagger & \mathbf{N}^\dagger\end{bmatrix} \begin{bmatrix}\mathbf{A}+\boldsymbol{\Delta} & \mathbf{B}+\boldsymbol{\Delta} & \mathbf{g}^\dagger & \tilde{\mathbf{g}}^\dagger \\ \mathbf{B}+\boldsymbol{\Delta} & \mathbf{A}+\boldsymbol{\Delta} & \mathbf{g}^\dagger & \tilde{\mathbf{g}}^\dagger \\ \mathbf{g} & \mathbf{g} & \boldsymbol{\omega} & 0 \\ \tilde{\mathbf{g}} & \tilde{\mathbf{g}} & 0 & \boldsymbol{\omega}\end{bmatrix} \begin{bmatrix}\mathbf{X} \\ \mathbf{Y} \\ \mathbf{M} \\ \mathbf{N}\end{bmatrix}^{[x]} \\ &= \Omega \begin{bmatrix}\mathbf{X}^\dagger & \mathbf{Y}^\dagger & \mathbf{M}^\dagger & \mathbf{N}^\dagger\end{bmatrix}^{[x]} \begin{bmatrix}\mathbf{X} \\ -\mathbf{Y} \\ \mathbf{M} \\ -\mathbf{N}\end{bmatrix} \\ &+ \Omega \begin{bmatrix}\mathbf{X}^\dagger & -\mathbf{Y}^\dagger & \mathbf{M}^\dagger & -\mathbf{N}^\dagger\end{bmatrix} \begin{bmatrix}\mathbf{X} \\ \mathbf{Y} \\ \mathbf{M} \\ \mathbf{N}\end{bmatrix}^{[x]} \\ &= \Omega \left(\mathbf{X}^\dagger\mathbf{X} - \mathbf{Y}^\dagger\mathbf{Y} + \mathbf{M}^\dagger\mathbf{M} - \mathbf{N}^\dagger\mathbf{N}\right)^{[x]} = 0\end{aligned} \tag{S41}$$

because each eigenvector of Eq. (S32) is normalized according to Eq. (3) of the main text.

The nuclear gradient, $\Omega^{[x]}$, of our TDDFT-PF energy in Eq. (S32) can be separated into the skeleton derivative, $\Omega^{[\tilde{x}]}$, and the orbital response term, $\Omega^{\mathbf{\Theta}} \cdot \mathbf{\Theta}^{[x]} = 2\mathcal{L} \cdot \mathbf{\Theta}^{[x]}$,

$$\begin{aligned}\Omega^{[x]} &= \Omega^{[\tilde{x}]} + \Omega^{\mathbf{\Theta}} \cdot \mathbf{\Theta}^{[x]} \\ &= \Omega^{[\widetilde{x}]} + \Omega^{\mathbf{S}} \cdot \mathbf{S}^{[x]} + \Omega^{\mathbf{\Theta}} \cdot \mathbf{\Theta}^{[x]} \\ &= \Omega^{\mathbf{III}} \cdot \mathbf{III}^{[\widetilde{x}]} + \mathbf{W} \cdot \mathbf{S}^{[x]} + 2\mathcal{L} \cdot \mathbf{\Theta}^{[x]}\end{aligned} \tag{S42}$$

where the skeleton derivative is further separated into the overlap derivative term, $\Omega^{\mathbf{S}} \cdot \mathbf{S}^{[x]} = \mathbf{W} \cdot \mathbf{S}^{[x]}$, and all other direct components ($\mathbf{III} = \mathbf{H}, \mathbf{\Pi}, \mathbf{F}^{\text{xc}}, \mathbf{\Omega}^{\text{xc}}, \mathbf{g}_{\text{ao}}$, and $\mathbf{\Delta}_{\text{ao}}$). Amongst, the core Hamiltonian ($\mathbf{H}$) contribution comes from Eq. (S39),

$$\Omega^{\mathbf{H}} \cdot \mathbf{H}^{[\widetilde{x}]} = \Omega^{\mathbf{H}} \cdot \mathbf{H}^{[x]} = \mathbf{P}_{\Delta} \cdot \mathbf{H}^{[x]} \tag{S43}$$

while the electron repulsion integral contributions arise also from Eq. (S40),

$$\Omega^{\mathbf{\Pi}} \cdot \mathbf{\Pi}^{[\widetilde{x}]} = \Omega^{\mathbf{\Pi}} \cdot \mathbf{\Pi}^{[x]} = \mathbf{\Gamma} \cdot \mathbf{\Pi}^{[x]}, \tag{S44}$$

$$\mathbf{\Gamma} = \mathbf{P}_{\Delta} \otimes \mathbf{P}_0 + \left(\mathbf{R}_X + \mathbf{R}_Y^{\dagger}\right) \otimes \left(\mathbf{R}_X + \mathbf{R}_Y^{\dagger}\right). \tag{S45}$$

The two exchange-correlation contributions are

$$\Omega^{\mathbf{F}^{\text{xc}}} \cdot (\mathbf{F}^{\text{xc}})^{[\widetilde{x}]} = \mathbf{P}_{\Delta} \cdot (\mathbf{F}^{\text{xc}})^{[\widetilde{x}]} \tag{S46}$$

$$\Omega^{\mathbf{\Omega}^{\text{xc}}} \cdot (\mathbf{\Omega}^{\text{xc}})^{[\widetilde{x}]} = \left(\mathbf{R}_X + \mathbf{R}_Y^{\dagger}\right) \cdot \left(\mathbf{\Omega}^{\text{xc}}\right)^{[\widetilde{x}]} \cdot \left(\mathbf{R}_X + \mathbf{R}_Y^{\dagger}\right) \tag{S47}$$

where $(\mathbf{F}^{\text{xc}})^{[\widetilde{x}]}$ and $\left(\mathbf{\Omega}^{\text{xc}}\right)^{[\widetilde{x}]}$ are direct derivatives of the exchange-correlation matrix in Eq. (S4) and the exchange-correlation portion of the response kernel in Eq. (S6), both excluding the orbital response and overlap contributions. The expressions for these two derivatives can be found in Eqs. 25 and 26 of Reference 1. For the DSE and electron-photon energy, the corresponding direct contributions are

$$\Omega^{\mathbf{\Delta}} \cdot \mathbf{\Delta}^{[\widetilde{x}]} = (\mathbf{R}_X + \mathbf{R}_Y) \cdot \mathbf{\Delta}_{\text{ao}}^{[x]} \cdot (\mathbf{R}_X + \mathbf{R}_Y) \tag{S48}$$

$$\Omega^{\mathbf{g}_{\text{ao}}} \cdot \mathbf{g}_{\text{ao}}^{[\widetilde{x}]} = 2\mathbf{G}^{[x]} \cdot (\mathbf{R}_X + \mathbf{R}_Y) \tag{S49}$$

where both $\mathbf{\Delta}_{\text{ao}}^{[x]}$ and $\mathbf{G}^{[x]}$ arise from the derivative of dipole matrix,

$$\mathbf{\Delta}_{\text{ao}}^{[x]} = 2\sum_{\alpha=1}^{M} \left(\boldsymbol{\mu}_{\text{ao}}^{[x]} \cdot \boldsymbol{\lambda}_{\alpha}\right) \otimes (\boldsymbol{\mu}_{\text{ao}} \cdot \boldsymbol{\lambda}_{\alpha}) \tag{S50}$$

$$\mathbf{G}^{[x]} = \sum_{\alpha} (M_{\alpha} + N_{\alpha}) \sqrt{\frac{\omega_{\alpha}}{2}} \left(\boldsymbol{\mu}_{\text{ao}}^{[x]} \cdot \boldsymbol{\lambda}_{\alpha}\right) \tag{S51}$$

For the overlap derivative of the electronic energy components in Eqs. (S39) and (S40), we can use Eq. (S25) to obtain

$$\begin{aligned}\mathbf{\Lambda}_{\text{ele},1} &= \mathbf{P}_{\Delta}\mathbf{F} + \mathbf{P}_0 \left[\mathbf{P}_{\Delta} \cdot \mathbf{F}^{\mathbf{P}_0}\right] \\ &= \mathbf{P}_{\Delta}\mathbf{F} + \mathbf{P}_0 \left[\left(\mathbf{\Pi} + \mathbf{\Omega}^{\text{xc}}\right) \cdot \mathbf{P}_{\Delta}\right]\end{aligned} \tag{S52}$$

$$\begin{aligned}\mathbf{\Lambda}_{\text{ele},2} &= \left(\mathbf{R}_X^{\dagger} + \mathbf{R}_Y\right) \left[\left(\mathbf{\Pi} + \mathbf{\Omega}^{\text{xc}}\right) \cdot \left(\mathbf{R}_X + \mathbf{R}_Y^{\dagger}\right)\right] \\ &\quad + \left(\mathbf{R}_X + \mathbf{R}_Y^{\dagger}\right) \left[\left(\mathbf{\Pi} + \mathbf{\Omega}^{\text{xc}}\right) \cdot \left(\mathbf{R}_X + \mathbf{R}_Y^{\dagger}\right)\right]^{\dagger} \\ &\quad + \mathbf{P}_0 \left[\left(\mathbf{R}_X + \mathbf{R}_Y^{\dagger}\right) \cdot \mathbf{\Xi}^{\text{xc}} \cdot \left(\mathbf{R}_X + \mathbf{R}_Y^{\dagger}\right)\right]\end{aligned} \tag{S53}$$

with the $\mathbf{\Xi}^{\text{xc}} = (\mathbf{\Omega}^{\text{xc}})^{\mathbf{P}_0}$ term involves the computation of functional third derivatives (see Eq. (S7)). Similarly, for the DSE and electron-photon energies in Eqs. (10) and (11) of the main text, we can obtain

$$\mathbf{\Lambda}_{\text{dse}} = (\mathbf{R}_X + \mathbf{R}_Y) \left[\mathbf{\Delta}_{\text{ao}} \cdot (\mathbf{R}_X + \mathbf{R}_Y)\right] \tag{S54}$$

$$\mathbf{\Lambda}_{\text{ele-ph}} = 2(\mathbf{R}_X + \mathbf{R}_Y)\mathbf{G} \tag{S55}$$

To obtain the orbital response term in the analytical gradient in Eq. (S42),

$$\Omega^{\boldsymbol{\Theta}} \cdot \boldsymbol{\Theta}^{[x]} = 2\boldsymbol{\mathcal{L}} \cdot \boldsymbol{\Theta}^{[x]} = 2 \sum_{ai} \mathcal{L}_{ai} \Theta_{ai}^{[x]}, \tag{S56}$$

one needs to compute the various components of the Lagrangian,

$$\mathcal{L}_{ai} = \frac{1}{2} \frac{\partial \Omega}{\partial \Theta_{ai}}. \tag{S57}$$

From Eqs. (S28) and (S29), the first electronic contribution to the Lagrangian are

$$\boldsymbol{\mathcal{L}}_{\text{ele},1} = \frac{1}{2} \mathbf{P}_0^{\boldsymbol{\Theta}} \cdot \left(\mathbf{F}^{\mathbf{P}_0} \cdot \mathbf{P}_{\boldsymbol{\Delta}} \right) = -\mathbf{C}_{\text{v}}^{\dagger} \left[\left(\boldsymbol{\Pi} + \boldsymbol{\Omega}^{\text{xc}} \right) \cdot \mathbf{P}_{\Delta} \right] \mathbf{C}_{\text{o}} \tag{S58}$$

while the second electronic contribution is (see lines 110–126 in libcp/makeal.F)

$$\begin{aligned}
\boldsymbol{\mathcal{L}}_{\text{ele},2} = & \left(\mathbf{R}_X + \mathbf{R}_Y^{\dagger} \right)^{\boldsymbol{\Theta}} \cdot \left(\boldsymbol{\Pi} + \boldsymbol{\Omega}^{\text{xc}} \right) \cdot \left(\mathbf{R}_X + \mathbf{R}_Y^{\dagger} \right) \\
& + \frac{1}{2} \left(\mathbf{R}_X + \mathbf{R}_Y^{\dagger} \right) \cdot \left(\boldsymbol{\Omega}^{\text{xc}} \right)^{\boldsymbol{\Theta}} \cdot \left(\mathbf{R}_X + \mathbf{R}_Y^{\dagger} \right) \\
= & \, \mathbf{X} \mathbf{C}_{\text{o}}^{\dagger} \left[\left(\boldsymbol{\Pi} + \boldsymbol{\Omega}^{\text{xc}} \right) \cdot \left(\mathbf{R}_X + \mathbf{R}_Y^{\dagger} \right) \right]^{\dagger} \mathbf{C}_{\text{o}} \\
& + \mathbf{Y} \mathbf{C}_{\text{o}}^{\dagger} \left[\left(\boldsymbol{\Pi} + \boldsymbol{\Omega}^{\text{xc}} \right) \cdot \left(\mathbf{R}_X + \mathbf{R}_Y^{\dagger} \right) \right] \mathbf{C}_{\text{o}} \\
& - \mathbf{C}_{\text{v}}^{\dagger} \left[\left(\boldsymbol{\Pi} + \boldsymbol{\Omega}^{\text{xc}} \right) \cdot \left(\mathbf{R}_X + \mathbf{R}_Y^{\dagger} \right) \right]^{\dagger} \mathbf{C}_{\text{v}} \mathbf{X} \\
& - \mathbf{C}_{\text{v}}^{\dagger} \left[\left(\boldsymbol{\Pi} + \boldsymbol{\Omega}^{\text{xc}} \right) \cdot \left(\mathbf{R}_X + \mathbf{R}_Y^{\dagger} \right) \right] \mathbf{C}_{\text{v}} \mathbf{Y} \\
& - \mathbf{C}_{\text{v}}^{\dagger} \left[\left(\mathbf{R}_X + \mathbf{R}_Y^{\dagger} \right) \cdot \boldsymbol{\Xi}^{\text{xc}} \cdot \left(\mathbf{R}_X + \mathbf{R}_Y^{\dagger} \right) \right] \mathbf{C}_{\text{o}}
\end{aligned} \tag{S59}$$

using Eqs. (S30) and (S31). Similarly, for the DSE and electron-photon energies in Eqs. (10) and (11), one has

$$\begin{aligned}
\boldsymbol{\mathcal{L}}_{\text{dse}} &= \left(\mathbf{R}_X + \mathbf{R}_Y \right)^{\boldsymbol{\Theta}} \cdot \boldsymbol{\Delta}_{\text{ao}} \cdot \left(\mathbf{R}_X + \mathbf{R}_Y \right) \\
&= \left(\mathbf{X} + \mathbf{Y} \right) \mathbf{C}_{\text{o}}^{\dagger} \left[\boldsymbol{\Delta}_{\text{ao}} \cdot \left(\mathbf{R}_X + \mathbf{R}_Y \right) \right]^{\dagger} \mathbf{C}_{\text{o}} \\
&\quad - \mathbf{C}_{\text{v}}^{\dagger} \left[\boldsymbol{\Delta}_{\text{ao}} \cdot \left(\mathbf{R}_X + \mathbf{R}_Y \right) \right]^{\dagger} \mathbf{C}_{\text{v}} \left(\mathbf{X} + \mathbf{Y} \right)
\end{aligned} \tag{S60}$$

and

$$\begin{aligned}
\boldsymbol{\mathcal{L}}_{\text{ele-ph}} &= \mathbf{G} \cdot \left(\mathbf{R}_X + \mathbf{R}_Y \right)^{\boldsymbol{\Theta}} \\
&= \left(\mathbf{X} + \mathbf{Y} \right) \mathbf{C}_{\text{o}}^{\dagger} \mathbf{G} \mathbf{C}_{\text{o}} - \mathbf{C}_{\text{v}}^{\dagger} \mathbf{G} \mathbf{C}_{\text{v}} \left(\mathbf{X} + \mathbf{Y} \right)
\end{aligned} \tag{S61}$$

3. *Efficient Gradient Evaluation with z-Vector*

A straightforward evaluation of the orbital response contribution to the TDDFT-PF gradient in Eq. (S56) would require $\boldsymbol{\Theta}^{[x]}$, a set of $3N_{\text{atom}}$ vectors that are solutions to the CPKS equations,

$$E^{\boldsymbol{\Theta}\boldsymbol{\Theta}} \cdot \boldsymbol{\Theta}^{[x]} = -E^{\boldsymbol{\Theta}\mathbf{S}} \cdot \mathbf{S}^{[x]} - E^{\boldsymbol{\Theta}\mathbf{III}} \cdot \mathbf{III}^{[\widetilde{x}]}. \tag{S62}$$

This expensive step can be mitigated by solving only for a single z-vector via Eq. (13) of the main text. Specifically, by writing the orbital responses as

$$\boldsymbol{\Theta}^{[x]} = -\left(E^{\boldsymbol{\Theta}\boldsymbol{\Theta}} \right)^{-1} \cdot \left[E^{\boldsymbol{\Theta}\mathbf{S}} \cdot \mathbf{S}^{[x]} + E^{\boldsymbol{\Theta}\mathbf{III}} \cdot \mathbf{III}^{[\widetilde{x}]} \right], \tag{S63}$$

one can reduce the orbital response term of the TDDFT-PF gradient in Eq. (S56) to

$$\begin{aligned} 2\boldsymbol{\mathcal{L}}\cdot\boldsymbol{\Theta}^{[x]} &= -2\boldsymbol{\mathcal{L}}\cdot\left(E^{\boldsymbol{\Theta}\boldsymbol{\Theta}}\right)^{-1}\cdot\left[E^{\boldsymbol{\Theta}\mathbf{S}}\cdot\mathbf{S}^{[x]}+E^{\boldsymbol{\Theta}\mathbf{III}}\cdot\mathbf{III}^{[\widetilde{x}]}\right] \\ &= -\mathbf{z}\cdot\left[E^{\boldsymbol{\Theta}\mathbf{S}}\cdot\mathbf{S}^{[x]}+E^{\boldsymbol{\Theta}\mathbf{III}}\cdot\mathbf{III}^{[\widetilde{x}]}\right] \end{aligned} \tag{S64}$$

Using Eq. (S28), one has

$$E^{\boldsymbol{\Theta}} = E^{\mathbf{P}_0}\cdot\mathbf{P}_0^{\boldsymbol{\Theta}} = \mathbf{F}\cdot\mathbf{P}_0^{\boldsymbol{\Theta}} = -\mathbf{C}_{\mathrm{v}}^{\dagger}\left(\mathbf{F}+\mathbf{F}^{\dagger}\right)\mathbf{C}_{\mathrm{o}}. \tag{S65}$$

Thus, for the first component in Eq. (S64), one has

$$\begin{aligned} -\mathbf{z}\cdot E^{\boldsymbol{\Theta}\mathbf{S}} &= -\left(\mathbf{z}\cdot E^{\boldsymbol{\Theta}}\right)^{\mathbf{S}} \\ &= \left(\mathbf{P}_z\cdot\mathbf{F}\right)^{\mathbf{S}} = \mathbf{P}_z^{\mathbf{S}}\cdot\mathbf{F}+\mathbf{P}_z\cdot\mathbf{F}^{\mathbf{S}} \end{aligned} \tag{S66}$$

where

$$\mathbf{P}_z^{\mathbf{S}}\cdot\mathbf{F} = -\frac{1}{2}\mathbf{P}_z\mathbf{F}\mathbf{C}\mathbf{C}^{\dagger}-\frac{1}{2}\mathbf{C}\mathbf{C}^{\dagger}\mathbf{F}\mathbf{P}_z \tag{S67}$$

$$\begin{aligned} \mathbf{P}_z\cdot\mathbf{F}^{\mathbf{S}} &= \mathbf{P}_z\cdot\mathbf{F}^{\mathbf{P}_0}\cdot\mathbf{P}_0^{\mathbf{S}} \\ &= \left[\left(\boldsymbol{\Pi}+\boldsymbol{\Omega}^{\mathrm{xc}}\right)\cdot\mathbf{P}_z\right]\cdot\mathbf{P}_0^{\mathbf{S}} \\ &= -\frac{1}{2}\mathbf{P}_0\left[\left(\boldsymbol{\Pi}+\boldsymbol{\Omega}^{\mathrm{xc}}\right)\cdot\mathbf{P}_z\right]\mathbf{C}\mathbf{C}^{\dagger} \\ &\quad -\frac{1}{2}\mathbf{C}\mathbf{C}^{\dagger}\left[\left(\boldsymbol{\Pi}+\boldsymbol{\Omega}^{\mathrm{xc}}\right)\cdot\mathbf{P}_z\right]\mathbf{P}_0 \end{aligned} \tag{S68}$$

Therefore,

$$-\mathbf{z}\cdot E^{\boldsymbol{\Theta}\mathbf{S}} = -\frac{1}{2}\boldsymbol{\Lambda}_z\mathbf{C}\mathbf{C}^{\dagger}-\frac{1}{2}\mathbf{C}\mathbf{C}^{\dagger}\boldsymbol{\Lambda}_z, \tag{S69}$$

where

$$\boldsymbol{\Lambda}_z = \mathbf{P}_z\mathbf{F}+\mathbf{P}_0\left[\left(\boldsymbol{\Pi}+\boldsymbol{\Omega}^{\mathrm{xc}}\right)\cdot\mathbf{P}_z\right] \tag{S70}$$

will be combined with Eq. (S52) to yield

$$\boldsymbol{\Lambda}'_{\mathrm{ele},1} = \mathbf{P}'_{\Delta}\mathbf{F}+\mathbf{P}_0\left[\left(\boldsymbol{\Pi}+\boldsymbol{\Omega}^{\mathrm{xc}}\right)\cdot\mathbf{P}'_{\Delta}\right]. \tag{S71}$$

Similarly, we can find other components of Eq. (S64) to be

$$-\mathbf{z}\cdot E^{\boldsymbol{\Theta}\mathbf{H}}\cdot\mathbf{H}^{[\widetilde{x}]} = \mathbf{P}_z\cdot\mathbf{H}^{[x]}, \tag{S72}$$

$$-\mathbf{z}\cdot E^{\boldsymbol{\Theta}\boldsymbol{\Pi}}\cdot\boldsymbol{\Pi}^{[\widetilde{x}]} = \left(\mathbf{P}_z\otimes\mathbf{P}_0\right)\cdot\boldsymbol{\Pi}^{[\widetilde{x}]}, \tag{S73}$$

$$-\mathbf{z}\cdot E^{\boldsymbol{\Theta}\mathbf{F}^{\mathrm{xc}}}\cdot\left(\mathbf{F}^{\mathrm{xc}}\right)^{[\widetilde{x}]} = \mathbf{P}_z\cdot\left(\mathbf{F}^{\mathrm{xc}}\right)^{[\widetilde{x}]}, \tag{S74}$$

which will be added to the corresponding terms in Eqs. (S43), (S44), and (S46), respectively.

S2. ETHYLENE MOLECULE

A. Ground-State Geometry of Ethylene Molecule Optimized Using the PBE0 Functional and 6-311++G** Basis Set

```
C2H4 PBE0 6-311++G**
6
-78.5042464024453
C  0.0000000000  0.6662105645  0.0000000000
C  0.0000000000 -0.6662105645  0.0000000000
H  0.0000000000  1.2386216337  0.9292861049
H  0.0000000000  1.2386216337 -0.9292861049
H  0.0000000000 -1.2386216337  0.9292861049
H  0.0000000000 -1.2386216337 -0.9292861049
```

B. TDDFT and cQED-TDDFT Results

TABLE S1. Composition of TDDFT-PF nonpolaritonic, lower and upper polaritonic states of ethylene within the optical cavity using the PBE0 functional and cc-pVDZ basis set. The expansion coefficients are computed as $C_k = \langle \Psi_k^{\text{vac}} | \Psi \rangle$.

State	NP	LP	UP
Index	2	1	3
Energy (eV)	8.237	8.026	8.312
C_0^2	0.0000	0.5289	0.4696
C_1^2	0.0000	0.4704	0.5296
C_2^2	1.0000	0.0000	0.0000
C_3^2	0.0000	0.0000	0.0000
C_4^2	0.0000	0.0000	0.0000
C_5^2	0.0000	0.0000	0.0000
C_6^2	0.0000	0.0000	0.0000
C_7^2	0.0000	0.0000	0.0000
C_8^2	0.0000	0.0000	0.0000
C_9^2	0.0000	0.0000	0.0000
C_{10}^2	0.0000	0.0005	0.0006

TABLE S2. Excitation energies (in eV) and transition dipole moments (in a.u.) of TDDFT excited states of gas-phase ethylene using the PBE0 functional and cc-pVDZ basis set.

State	Energy	x	y	z
1	8.173	-0.000	1.360	-0.000
2	8.237	0.000	0.000	0.000
3	8.644	-0.309	-0.000	-0.000
4	9.146	0.000	0.000	-0.000
5	9.590	-0.000	-0.000	-0.000
6	9.826	0.000	-0.000	0.000
7	10.865	-0.000	0.000	-0.000
8	11.248	-0.000	-0.000	-0.000
9	11.611	-0.000	-0.000	0.000
10	11.748	-0.000	1.106	0.000

TABLE S3. Gradients (in a.u.) of ground-state and first TDDFT excited state of gas-phase ethylene molecule using the PBE0 functional and cc-pVDZ basis set. Also shown are the linear combinations.

Atom	x	y	z	x	y	z
		Ground-state ($E_0^{[x]}$)			First excited-state ($E_1^{[x]}$)	
C	-0.0000000	0.0034322	0.0000000	0.0000000	-0.1804117	-0.0000000
C	0.0000000	-0.0034322	0.0000000	0.0000000	0.1804117	0.0000000
H	0.0000000	-0.0007447	-0.0013775	-0.0000000	-0.0023960	-0.0003592
H	0.0000000	-0.0007447	0.0013775	0.0000000	-0.0023960	0.0003592
H	0.0000000	0.0007447	-0.0013775	0.0000000	0.0023960	-0.0003592
H	-0.0000000	0.0007447	0.0013775	-0.0000000	0.0023960	0.0003592
		$0.5289\,E_0^{[x]} + 0.4704\,E_1^{[x]}$			$E_{\mathrm{LP}}^{[x]} - 0.5289\,E_0^{[x]} - 0.4704\,E_1^{[x]}$	
C	0.0000000	-0.0830588	-0.0000000	-0.0000000	-0.0004198	-0.0000000
C	0.0000000	0.0830588	0.0000000	-0.0000000	0.0004198	0.0000000
H	-0.0000000	-0.0015211	-0.0008975	0.0000000	-0.0000180	-0.0000477
H	0.0000000	-0.0015211	0.0008975	-0.0000000	-0.0000180	0.0000477
H	0.0000000	0.0015211	-0.0008975	-0.0000000	0.0000180	-0.0000477
H	-0.0000000	0.0015211	0.0008975	0.0000000	0.0000180	0.0000477
		$0.4696\,E_0^{[x]} + 0.5296\,E_1^{[x]}$			$E_{\mathrm{UP}}^{[x]} - 0.4696\,E_0^{[x]} - 0.5296\,E_1^{[x]}$	
C	-0.0000000	-0.0939389	-0.0000000	0.0000000	0.0007306	0.0000000
C	-0.0000000	0.0939389	0.0000000	0.0000000	-0.0007306	-0.0000000
H	-0.0000000	-0.0016187	-0.0008371	0.0000000	-0.0001382	-0.0000536
H	0.0000000	-0.0016187	0.0008371	-0.0000000	-0.0001382	0.0000536
H	0.0000000	0.0016187	-0.0008371	-0.0000000	0.0001382	-0.0000536
H	-0.0000000	0.0016187	0.0008371	0.0000000	0.0001382	0.0000536

C. Optimized Geometry for Lower and Upper Polaritons

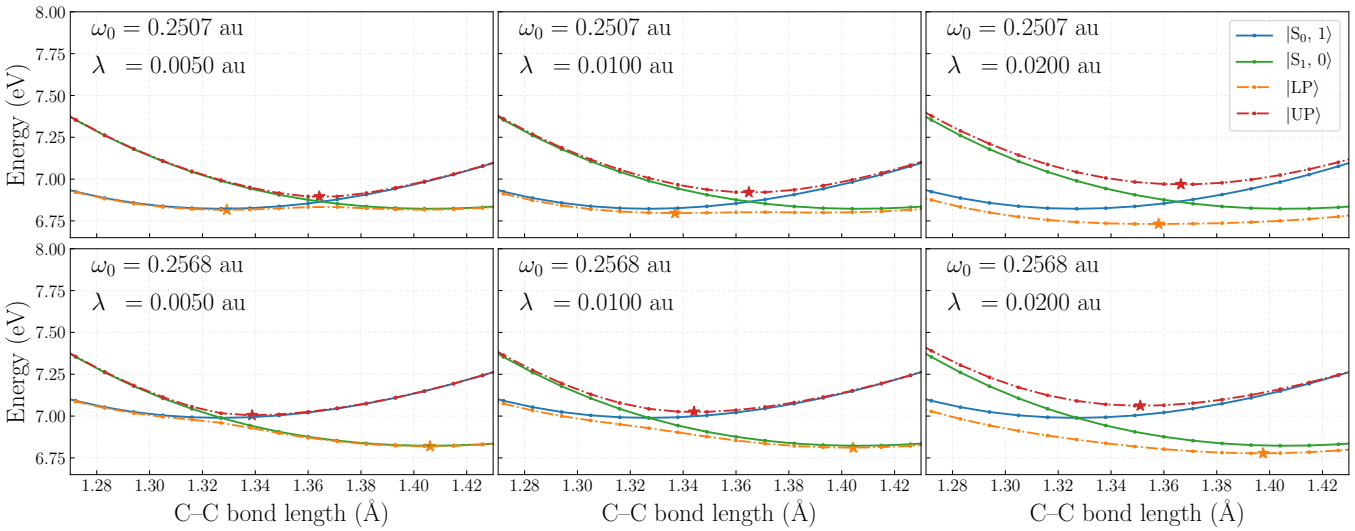

FIG. S1. Potential energy curves of a single ethylene molecule scanned with respect to C–C bond lengths. Optimized C–C bond lengths are marked with stars for upper and lower polaritons of ethylene molecule coupled to a single cavity mode from TDA-JC model calculations with the PBE0 functional and 6-311++G** basis set, using the analytic gradient developed in this work. The photon E-field is aligned with the transition dipole moment of the first excited state, which is perpendicular to the molecule. The photon energy is 0.2507 au, which is equal to the gas-phase adiabatic excitation energy, in the top three panels; while it is set to be 0.2568 au, which corresponds to the gas-phase vertical excitation energy, in the lower three panels. The coupling strengths are set to 0.005, 0.01, and 0.02 au. Note that, due to vibronic decoupling,[17–19] such geometry optimization is ***not*** directly applicable to the molecule in a reduced CIS-TC model (Eq. (23) in the main text), where the electron–photon coupling is scaled by $\sqrt{N}$ (or $\sqrt{N/3}$) to capture a collective excitation among N parallel (or randomly-oriented) molecules.

S3. BENZALDEHYDE MOLECULE

A. Ground-State Geometry of Benzaldehyde Molecule Optimized Using the PBE0 Functional and 6-311++G** Basis Set

```
C6H5CHO PBE0 6-311++G**
14
-345.255583702600
C    0.0444176449 -1.1018291187 0.0000000000
C   -1.3261410267 -1.3281816235 0.0000000000
C   -2.2133752765 -0.2471903340 0.0000000000
C   -1.7312839975  1.0611346821 0.0000000000
C   -0.3570221851  1.2888292340 0.0000000000
C    0.5334742585  0.2107166850 0.0000000000
C    1.9887836264  0.4668394275 0.0000000000
O    2.8410453615 -0.3945408322 0.0000000000
H   -1.7117538780 -2.3482451649 0.0000000000
H   -3.2892064941 -0.4282442776 0.0000000000
H   -2.4267559760  1.9009365066 0.0000000000
H    0.0335635546  2.3089090226 0.0000000000
H    2.2739453181  1.5465885188 0.0000000000
H    0.7587263192 -1.9255316626 0.0000000000
```

B. QED-TDDFT Results

TABLE S4. Energy (in eV) and photon character of the first non-polaritonic (NP) and the first two polaritonic states of benzaldehyde with various cavity methods, functionals, and basis sets. Hopefield populations are enclosed in the round brackets.

Cavity	State	cc-pVDZ			aug-cc-pVDZ		
		HF	PBE0	PBE	HF	PBE0	PBE
TDA-JC	NP	4.667 (0.000)	3.635 (0.000)	3.144 (0.000)	4.695 (0.000)	3.620 (0.000)	3.135 (0.000)
	P1	7.383 (0.519)	5.460 (0.566)	5.110 (0.567)	5.577 (0.588)	5.252 (0.569)	4.890 (0.583)
	P2	7.844 (0.340)	5.715 (0.420)	5.349 (0.420)	5.762 (0.370)	5.509 (0.415)	5.113 (0.378)
TDA-RWA	NP	4.667 (0.000)	3.635 (0.000)	3.144 (0.000)	4.695 (0.000)	3.620 (0.000)	3.135 (0.000)
	P1	7.392 (0.535)	5.465 (0.577)	5.114 (0.578)	5.580 (0.594)	5.256 (0.581)	4.894 (0.594)
	P2	7.848 (0.314)	5.717 (0.409)	5.351 (0.409)	5.763 (0.363)	5.511 (0.403)	5.114 (0.367)
TDA-Rabi	NP	4.667 (0.000)	3.635 (0.000)	3.144 (0.000)	4.695 (0.000)	3.620 (0.000)	3.135 (0.000)
	P1	7.381 (0.515)	5.459 (0.563)	5.109 (0.564)	5.577 (0.586)	5.250 (0.566)	4.889 (0.580)
	P2	7.843 (0.347)	5.715 (0.423)	5.349 (0.423)	5.762 (0.372)	5.509 (0.418)	5.112 (0.380)
TDA-PF	NP	4.667 (0.000)	3.635 (0.000)	3.144 (0.000)	4.695 (0.000)	3.620 (0.000)	3.135 (0.000)
	P1	7.390 (0.531)	5.463 (0.574)	5.113 (0.575)	5.580 (0.593)	5.255 (0.578)	4.893 (0.591)
	P2	7.847 (0.320)	5.717 (0.412)	5.351 (0.412)	5.763 (0.365)	5.510 (0.406)	5.114 (0.370)
TDDFT-JC	NP	4.497 (0.000)	3.609 (0.000)	3.128 (0.000)	4.528 (0.000)	3.595 (0.000)	3.119 (0.000)
	P1	6.953 (0.528)	5.212 (0.573)	4.858 (0.573)	6.678 (0.531)	5.030 (0.578)	4.678 (0.580)
	P2	7.343 (0.315)	5.442 (0.416)	5.075 (0.419)	7.058 (0.278)	5.264 (0.410)	4.897 (0.407)
TDDFT-RWA	NP	4.497 (0.000)	3.609 (0.000)	3.128 (0.000)	4.528 (0.000)	3.595 (0.000)	3.119 (0.000)
	P1	6.959 (0.543)	5.216 (0.584)	4.862 (0.583)	6.685 (0.546)	5.034 (0.589)	4.682 (0.591)
	P2	7.346 (0.288)	5.444 (0.406)	5.077 (0.408)	7.060 (0.255)	5.266 (0.399)	4.898 (0.396)
TDDFT-Rabi	NP	4.497 (0.000)	3.609 (0.000)	3.128 (0.000)	4.528 (0.000)	3.595 (0.000)	3.119 (0.000)
	P1	6.951 (0.525)	5.211 (0.571)	4.857 (0.570)	6.676 (0.527)	5.029 (0.575)	4.677 (0.577)
	P2	7.342 (0.321)	5.442 (0.419)	5.075 (0.421)	7.057 (0.284)	5.264 (0.413)	4.896 (0.410)
TDDFT-PF	NP	4.497 (0.000)	3.609 (0.000)	3.128 (0.000)	4.528 (0.000)	3.595 (0.000)	3.119 (0.000)
	P1	6.958 (0.539)	5.215 (0.581)	4.861 (0.581)	6.683 (0.542)	5.033 (0.586)	4.681 (0.588)
	P2	7.345 (0.295)	5.443 (0.408)	5.077 (0.411)	7.060 (0.261)	5.265 (0.402)	4.898 (0.399)

TABLE S5. Root mean square differences (RMSD, in a.u.) between analytic and numerical gradient of the first non-polaritonic (NP) and the first two polaritonic states of benzaldehyde with various cavity methods, functionals, and basis sets. Numerical gradients were evaluated using a step size of 1.0×10^{-4} a_0.

Cavity	State	cc-pVDZ			aug-cc-pVDZ		
		HF	PBE0	PBE	HF	PBE0	PBE
TDA-JC	NP	0.00000002	0.00000050	0.00000053	0.00000003	0.00000060	0.00000111
	P1	0.00000001	0.00000048	0.00000059	0.00000003	0.00000058	0.00000057
	P2	0.00000001	0.00000048	0.00000059	0.00000003	0.00000062	0.00000060
TDA-RWA	NP	0.00000002	0.00000050	0.00000053	0.00000003	0.00000060	0.00000111
	P1	0.00000001	0.00000048	0.00000059	0.00000003	0.00000058	0.00000056
	P2	0.00000001	0.00000048	0.00000059	0.00000003	0.00000062	0.00000061
TDA-Rabi	NP	0.00000002	0.00000050	0.00000053	0.00000003	0.00000060	0.00000111
	P1	0.00000001	0.00000048	0.00000059	0.00000003	0.00000058	0.00000057
	P2	0.00000001	0.00000048	0.00000059	0.00000003	0.00000062	0.00000060
TDA-PF	NP	0.00000002	0.00000050	0.00000053	0.00000003	0.00000060	0.00000111
	P1	0.00000001	0.00000048	0.00000059	0.00000003	0.00000058	0.00000057
	P2	0.00000001	0.00000048	0.00000059	0.00000003	0.00000062	0.00000061
TDDFT-JC	NP	0.00000003	0.00000050	0.00000053	0.00000015	0.00000060	0.00000111
	P1	0.00000001	0.00000049	0.00000059	0.00000005	0.00000057	0.00000058
	P2	0.00000002	0.00000049	0.00000060	0.00000014	0.00000060	0.00000058
TDDFT-RWA	NP	0.00000003	0.00000050	0.00000053	0.00000019	0.00000060	0.00000111
	P1	0.00000001	0.00000049	0.00000059	0.00000004	0.00000057	0.00000057
	P2	0.00000001	0.00000049	0.00000060	0.00000011	0.00000061	0.00000059
TDDFT-Rabi	NP	0.00000003	0.00000050	0.00000053	0.00000009	0.00000060	0.00000111
	P1	0.00000001	0.00000049	0.00000059	0.00000003	0.00000057	0.00000058
	P2	0.00000001	0.00000048	0.00000060	0.00000007	0.00000061	0.00000058
TDDFT-PF	NP	0.00000003	0.00000050	0.00000053	0.00000016	0.00000060	0.00000111
	P1	0.00000001	0.00000049	0.00000059	0.00000004	0.00000057	0.00000057
	P2	0.00000001	0.00000049	0.00000060	0.00000010	0.00000061	0.00000058

S4. ANTHRACENE MOLECULES

A. Geometry of Anthracene Mononer from the Crystal Structure

C14H10
24

C	0.2563736	3.7093242	-0.0449170
C	0.5661749	2.6600202	-0.8759363
C	0.2797705	1.3088920	-0.4472129
C	0.5792674	0.2032321	-1.2704153
C	-0.3070134	1.1003717	0.8329083
C	-0.6166401	2.2409959	1.6556819
C	-0.3421122	3.4996589	1.2157780
H	0.4571640	4.7262713	-0.5058270
H	1.0831985	2.7719441	-1.8914144
H	1.0162632	0.3794854	-2.2827959
H	-1.0014252	2.0088645	2.6893248
H	-0.5448425	4.2520931	2.1112237
C	0.3070134	-1.1003717	-0.8329083
C	-0.5792674	-0.2032321	1.2704153
C	-0.2797705	-1.3088920	0.4472129
C	0.6166401	-2.2409959	-1.6556819
H	-1.0162632	-0.3794854	2.2827959
C	-0.5661749	-2.6600202	0.8759363
C	0.3421122	-3.4996589	-1.2157780
H	1.0014252	-2.0088645	-2.6893248
C	-0.2563736	-3.7093242	0.0449170
H	-1.0831985	-2.7719441	1.8914144
H	0.5448425	-4.2520931	-2.1112237
H	-0.4571640	-4.7262713	0.5058270

B. Geometry of Anthracene Dimer from the Crystal Structure

C28H20
48

C	0.2563736	3.7093242	-0.0449170
C	0.5661749	2.6600202	-0.8759363
C	0.2797705	1.3088920	-0.4472129
C	0.5792674	0.2032321	-1.2704153
C	-0.3070134	1.1003717	0.8329083
C	-0.6166401	2.2409959	1.6556819
C	-0.3421122	3.4996589	1.2157780
H	0.4571640	4.7262713	-0.5058270
H	1.0831985	2.7719441	-1.8914144
H	1.0162632	0.3794854	-2.2827959
H	-1.0014252	2.0088645	2.6893248
H	-0.5448425	4.2520931	2.1112237
C	0.3070134	-1.1003717	-0.8329083
C	-0.5792674	-0.2032321	1.2704153
C	-0.2797705	-1.3088920	0.4472129
C	0.6166401	-2.2409959	-1.6556819
H	-1.0162632	-0.3794854	2.2827959
C	-0.5661749	-2.6600202	0.8759363
C	0.3421122	-3.4996589	-1.2157780
H	1.0014252	-2.0088645	-2.6893248
C	-0.2563736	-3.7093242	0.0449170
H	-1.0831985	-2.7719441	1.8914144
H	0.5448425	-4.2520931	-2.1112237
H	-0.4571640	-4.7262713	0.5058270
C	0.1300580	3.9115478	-6.0782105
C	0.4398595	2.8622435	-6.9092207
C	0.1534549	1.5111156	-6.4805064
C	0.4529518	0.4054558	-7.3037088
C	-0.4333289	1.3025950	-5.2003762
C	-0.7429555	2.4432193	-4.3776025
C	-0.4684278	3.7018826	-4.8175155
H	0.3308486	4.9284946	-6.5391115
H	0.9568829	2.9741678	-7.9247079
H	0.8899478	0.5817087	-8.3160804
H	-1.1277408	2.2110881	-3.3439687
H	-0.6711581	4.4543168	-3.9220698
C	0.1806978	-0.8981481	-6.8662018
C	-0.7055828	-0.0010088	-4.7628692
C	-0.4060859	-1.1066686	-5.5860716
C	0.4903245	-2.0387723	-7.6889754
H	-1.1425788	-0.1772617	-3.7504976
C	-0.6924905	-2.4577965	-5.1573572
C	0.2157966	-3.2974353	-7.2490715
H	0.8751096	-1.8066408	-8.7226183
C	-0.3826892	-3.5071005	-5.9883765
H	-1.2095141	-2.5697205	-4.1418791
H	0.4185269	-4.0498695	-8.1445172
H	-0.5834796	-4.5240476	-5.5274665

C. Geometry of Anthracen Trimer from the Crystal Structure

C42H30
72

C	0.2563736	3.7093242	-0.0449170
C	0.5661749	2.6600202	-0.8759363
C	0.2797705	1.3088920	-0.4472129
C	0.5792674	0.2032321	-1.2704153
C	-0.3070134	1.1003717	0.8329083
C	-0.6166401	2.2409959	1.6556819
C	-0.3421122	3.4996589	1.2157780
H	0.4571640	4.7262713	-0.5058270
H	1.0831985	2.7719441	-1.8914144
H	1.0162632	0.3794854	-2.2827959
H	-1.0014252	2.0088645	2.6893248
H	-0.5448425	4.2520931	2.1112237
C	0.3070134	-1.1003717	-0.8329083
C	-0.5792674	-0.2032321	1.2704153
C	-0.2797705	-1.3088920	0.4472129
C	0.6166401	-2.2409959	-1.6556819
H	-1.0162632	-0.3794854	2.2827959
C	-0.5661749	-2.6600202	0.8759363
C	0.3421122	-3.4996589	-1.2157780
H	1.0014252	-2.0088645	-2.6893248
C	-0.2563736	-3.7093242	0.0449170
H	-1.0831985	-2.7719441	1.8914144
H	0.5448425	-4.2520931	-2.1112237
H	-0.4571640	-4.7262713	0.5058270
C	0.1300580	3.9115478	-6.0782105
C	0.4398595	2.8622435	-6.9092207
C	0.1534549	1.5111156	-6.4805064
C	0.4529518	0.4054558	-7.3037088
C	-0.4333289	1.3025950	-5.2003762
C	-0.7429555	2.4432193	-4.3776025
C	-0.4684278	3.7018826	-4.8175155
H	0.3308486	4.9284946	-6.5391115
H	0.9568829	2.9741678	-7.9247079
H	0.8899478	0.5817087	-8.3160804
H	-1.1277408	2.2110881	-3.3439687
H	-0.6711581	4.4543168	-3.9220698
C	0.1806978	-0.8981481	-6.8662018
C	-0.7055828	-0.0010088	-4.7628692
C	-0.4060859	-1.1066686	-5.5860716
C	0.4903245	-2.0387723	-7.6889754
H	-1.1425788	-0.1772617	-3.7504976
C	-0.6924905	-2.4577965	-5.1573572
C	0.2157966	-3.2974353	-7.2490715
H	0.8751096	-1.8066408	-8.7226183
C	-0.3826892	-3.5071005	-5.9883765
H	-1.2095141	-2.5697205	-4.1418791
H	0.4185269	-4.0498695	-8.1445172
H	-0.5834796	-4.5240476	-5.5274665
C	0.3826892	3.5071005	5.9883765
C	0.6924905	2.4577965	5.1573572
C	0.4060859	1.1066686	5.5860716
C	0.7055828	0.0010088	4.7628692
C	-0.1806978	0.8981481	6.8662018

```
C   -0.4903245    2.0387723    7.6889754
C   -0.2157966    3.2974353    7.2490715
H    0.5834796    4.5240476    5.5274665
H    1.2095141    2.5697205    4.1418791
H    1.1425788    0.1772617    3.7504976
H   -0.8751096    1.8066408    8.7226183
H   -0.4185269    4.0498695    8.1445172
C    0.4333289   -1.3025950    5.2003762
C   -0.4529518   -0.4054558    7.3037088
C   -0.1534549   -1.5111156    6.4805064
C    0.7429555   -2.4432193    4.3776025
H   -0.8899478   -0.5817087    8.3160804
C   -0.4398595   -2.8622435    6.9092207
C    0.4684278   -3.7018826    4.8175155
H    1.1277408   -2.2110881    3.3439687
C   -0.1300580   -3.9115478    6.0782105
H   -0.9568829   -2.9741678    7.9247079
H    0.6711581   -4.4543168    3.9220698
H   -0.3308486   -4.9284946    6.5391115
```

REFERENCES

[1] F. Liu, Z. Gan, Y. Shao, C.-P. Hsu, A. Dreuw, M. Head-Gordon, B. T. Miller, B. R. Brooks, J.-G. Yu, T. R. Furlani, and J. Kong, "A Parallel Implementation of the Analytic Nuclear Gradient for Time-Dependent Density Functional Theory within the Tamm-Dancoff Approximation," Mol. Phys. **108**, 2791–2800 (2010).

[2] M. E. Casida, "Time-Dependent Density-Functional Response Theory for Molecules," in *Recent Advances in Density Functional Methods Part I.* (World Scientific, 1995) p. 155.

[3] R. Bauernschmitt and R. Ahlrichs, "Treatment of Electronic Excitations within the Adiabatic Approximation of Time Dependent Density Functional Theory," Chem. Phys. Lett. **256**, 454–464 (1996).

[4] S. Hirata and M. Head-Gordon, "Time-Dependent Density Functional Theory within the Tamm-Dancoff Approximation," Chem. Phys. Lett. **314**, 291–299 (1999).

[5] A. Dreuw and M. Head-Gordon, "Single-Reference ab Initio Methods for the Calculation of Excited States of Large Molecules," Chem. Rev. **105**, 4009–4037 (2005).

[6] M. E. Casida, "Time-Dependent Density-Functional Theory for Molecules and Molecular Solids," J. Mol. Struct. THEOCHEM **914**, 3–18 (2009).

[7] M. Casida and M. Huix-Rotllant, "Progress in Time-Dependent Density-Functional Theory," Ann. Rev. Phys. Chem. **63**, 287–323 (2012).

[8] G. P. Chen, V. K. Voora, M. M. Agee, S. G. Balasubramani, and F. Furche, "Random-Phase Approximation Methods," Annu. Rev. Phys. Chem. **68**, 421–445 (2017).

[9] C. Schäfer, M. Ruggenthaler, and A. Rubio, "*Ab Initio* nonrelativistic quantum electrodynamics: Bridging quantum chemistry and quantum optics from weak to strong coupling," Phys. Rev. A **98**, 043801 (2018).

[10] J. Flick, D. M. Welakuh, M. Ruggenthaler, H. Appel, and A. Rubio, "Light–Matter Response in Nonrelativistic Quantum Electrodynamics," ACS Photonics **6**, 2757–2778 (2019).

[11] J. Yang, Q. Ou, Z. Pei, H. Wang, B. Weng, Z. Shuai, K. Mullen, and Y. Shao, "Quantum-electrodynamical time-dependent density functional theory within Gaussian atomic basis," J. Chem. Phys. **155**, 064107 (2021).

[12] A. Mandal, T. D. Krauss, and P. Huo, "Polariton-Mediated Electron Transfer via Cavity Quantum Electrodynamics," J. Phys. Chem. B **124**, 6321–6340 (2020).

[13] T. S. Haugland, C. Schäfer, E. Ronca, A. Rubio, and H. Koch, "Intermolecular interactions in optical cavities: An ab initio QED study," J. Chem. Phys. **154**, 094113 (2021).

[14] Y. Yamaguchi, J. Goddard, Y. Osamura, and H. Schaefer III, *A New Dimension to Quantum Chemistry: Analytic Derivative Methods in Ab Initio Molecular Electronic Structure Theory*, International Series of Monographs on Chemistry No. 29 (Oxford University Press, 1994).

[15] D. Maurice and M. Head-Gordon, "Analytical Second Derivatives for Excited Electronic States Using the Single Excitation Configuration Interaction Method: Theory and Application to Benzo[a]pyrene and Chalcone," Mol. Phys. **96**, 1533–1541 (1999).

[16] N. Bellonzi, G. R. Medders, E. Epifanovsky, and J. E. Subotnik, "Configuration interaction singles with spin-orbit coupling: Constructing spin-adiabatic states and their analytical nuclear gradients," J. Chem. Phys. **150**, 014106 (2019).

[17] F. C. Spano, "Optical Microcavities Enhance the Exciton Coherence Length and Eliminate Vibronic Coupling in J-aggregates," J. Chem. Phys. **142**, 184707 (2015).

[18] F. Herrera and F. C. Spano, "Cavity-Controlled Chemistry in Molecular Ensembles," Phys. Rev. Lett. **116**, 238301 (2016).

[19] J. Galego, F. J. Garcia-Vidal, and J. Feist, "Suppressing photochemical reactions with quantized light fields," Nat. Commun. **7**, 13841 (2016).